PHOTORESPONSE IN WIDE ELECTRODE SPACING PLANAR METAL-SEMICONDUCTOR-METAL PHOTODIODES STRUCTURES

การตอบสนองทางแสงที่บริเวณระหว่างขั้วไฟฟ้ากว้างมากของโฟโตไดโอดโครงสร้างเชิงราบโลหะ-สารกึ่งตัวนำ-โลหะ

Sanya Khunkhao
Department of Electrical Engineering
Faculty of Engineering, Sripatum University
E-mail : sanya.kh@spu.ac.th

Kazunori SATO
Department of Information
School of Information Science and Technology,
Tokai University
E-mail : kznrsato@keyaki.cc.u-tokai.ac.jp

ABSTRACT

The lateral spreading along surface of space-charge-region (SCR) of wide electrode spacing planar metal-semiconductor-metal (MSM) structures has been investigated. Planar MSM structures have been attracted much attention as viable optical sensor structures. For this purpose, the SCR of such a structure plays a key role in generating photocurrent in dc (static) the wider SCR along the active surface is the better from the efficiency point of view. To study the bias-controllable of photocurrent of the SCR along the surface of MSM structures, we prepared planar MSM structure with a wide electrode separation. We examined their SCR spreading through the photocurrent-bias voltage characteristics. The experimental results were compared with the numerical simulation using a quasi -1D model of such a planar structure. It was confirmed that, in addition to the existing photosensing function, output photocurrent of such a structure could be controlled by applying bias via lateral spreading of the surface space-charge-region (SCR) in the reverse-biased Schottky junction.

KEYWORDS : Metal-semiconductor-metal structure, Schottky barriers, Depletion region

บทคัดย่อ

การแผ่ขยายออกของบริเวณปลอดพาหะ (SCR) ตามแนวราบที่อยู่ระหว่างขั้วโลหะที่กว้างมาก ที่เป็นโครงสร้างเชิงราบโลหะ-สารกึ่งตัวนำ-โลหะ โดยที่ตัวตัวจับแสงโครงสร้างเชิงราบนี้เป็นที่ได้รับความสนใจอย่างมากในการเป็นตัวตรวจจับแสง โดยบริเวณปลอดพาหะเป็นส่วนสำคัญในกระแสแสงที่กำเนิดขึ้นภายใต้การควบคุมด้วยแรงดันไบอัส การวิจัยนี้ได้นำเสนอถึงกระแสแสงที่กำเนิดขึ้นตรงบริเวณปลอดพาหะ (SCR) ที่ขยายเพิ่มขึ้นด้วยแรงดันไบอัสที่อยู่ระหว่างอยู่ระหว่างขั้วโลหะโครงสร้าง MSM ที่กว้างมาก ด้วยสมบัติระหว่างกระแสแสงกับแรงดันไบอัส จากผลการทดสอบการแผ่ขยายของบริเวณปลอดพาหะ สามารถยืนยันด้วยแบบจำลองคำนวณหนึ่งมิติ ซึ่งผลการตอบสนองของกระแสแสงขึ้นกับแรงดันไบแอสทำให้บริเวณปลอดพาหะแผ่ขยายออกตามแนวราบที่ผิวหน้า ซึ่งเป็นรอยต่อช็อตคีย์ที่แรงดันย้อนกลับ

คำสำคัญ : โครงสร้างโลหะ-สารกึ่งตัวนำ-โลหะ รอยต่อช็อตคีย์ บริเวณปลอดพาหะ

Introduction

With a recent increasing demand of optical signal processing, there has been a stable research interest in the development of optical sensor devices in the form of planar rectifying metal-semiconductor-metal photodetector (MSM-PD) structures (Berger, 1996), (Seto, et al., 1997) and (Averine, et al., 2001). The MSM-PD structure has Schottky-barriers on both sides of the active region, where there must be the so-called space-charge region (SCR) contributing to the photocurrent generation (Berger, 1996). To achieve an efficient photocurrent generation in the MSM-PD structures, the larger active area is the better. However, in case of meeting higher frequency operation, the narrower SCR is desired to reduce the transit-time of carriers. That is, the lateral spreading of the SCR is one of the trade-off problems for MSM-PD structures. As one of the solutions of this problem, an interdigitated MSM structure has been investigated intensively (Averine, et al., 2001), (Masui, et al., 2003) and (Takano, et al., 2000). Thus, the laterally extending of the SCR exposed to optical illumination to be detected is essentially important. We proposed a simple model for the lateral spreading of the SCR of MSM-PD structures (Masui, et al., 2003).

A planar metal-semiconductor-metal (MSM) structure is simply composed of two back-to-back or face-to-face Schottky barriers placed flatwise and it has some advantages as a viable photosensing structure. One of them is the feasibility of fabricating optoelectronic integrated circuits (OEICs) (Harder, et al., 1990). Because of its simple and compatible fabrication process such as forming Schottky barrier of MSM structure, the process is essentially identical to the gate metallization of field effect transistors (FETs). Moreover, although there may be design trade-offs for optimizing between speed and efficiency, such a structure could have lower capacitance and be often transit-time-limited to meet wide band operation (Wei, et al., 1990). In this study, Si-based planar MSM photosensing structures were treated comparison between the experimental results and the simulations.

Experimental

1. Sample Preparation

The test samples have planar molybdenum/n-type semiconductor/molybdenum (Mo/n-Si/Mo) structure

prepared by following process. This structure has Schottky barrier junction between evaporated molybdenum and n-type silicon. Electron-beam evaporation of molybdenum was carried out onto an n-type mirror polished surface of silicon of resistivity (9-12) Ω-cm, which had been cleaned chemically and then rinsed by deionized (DI) water in ultrasonic bath beforehand. The thickness of deposited molybdenum film was approximately 3000 Å. Molybdenum film so formed works as Schottky barrier metal and electrodes as well. Figure 1 (a) illustrates the cross-sectional configuration of the sample, which was completed using photolithographic lift-off technique. Figure 1 (b), under a bias, the anode is forward-biased and the cathode is reversed-biased.

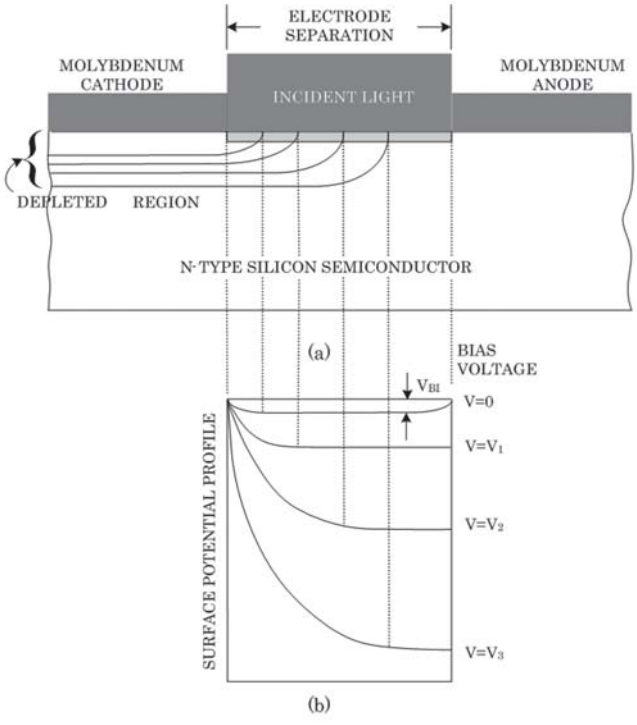

Figure 1 Schematic illustration of cross-sectional view of the test device with depletion layer (a) and potential profiles under various bias voltages (b). In the potential profiles, Schottky effect at cathode edge and depletion layer of anode forward-biased are ignored.

The configuration is symmetrical and the size of two electrodes is the same and of $3mm \times 3mm$. The electrode separation is 20 μm to 2000 μm. No particular anti-reflection coating was made onto the photo sensing area between the electrodes. The scanning electron microscope (SEM) image of the experimental samples used in this study is shown in Fig. 2. These values of the electrode separation are larger than the expected width of the SCR along the front surface, resulting in leaving the undepleted region. The structure is face-to-face structure of two Schottky junctions. The sample is not interdigitated but of single slit type. The internal separation between the electrodes is 20 μm, which is wide enough for the depleted region of both junctions not to get touch with one another even when bias voltage is applied.

Thus, the band diagram of the structure under a bias much larger than its built-in voltage is assumed a single junction. From the forward current-voltage (I-V) characteristics and capacitance-voltage (C-V) characteristics under dark of independent Schottky-barriers, the barrier height and built-in voltage were estimated to lie around 0.70 eV and 0.23 eV, respectively (1).

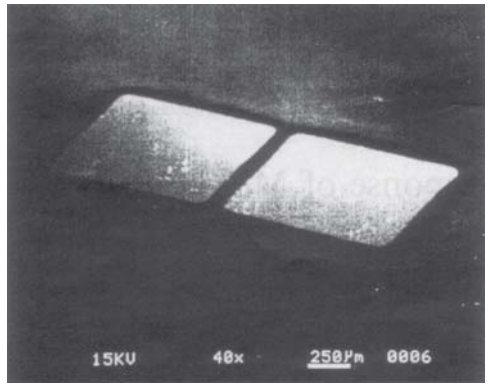

Figure 2 SEM image of a sample with 100 μm electrode separation (before bonding)

2. Measurement Procedure

The current versus applied bias (I-V) characteristics were measured under optical illumination and in the dark conditions. The block diagram of the set up for measurements of I-V characteristics is shown in Fig. 3.

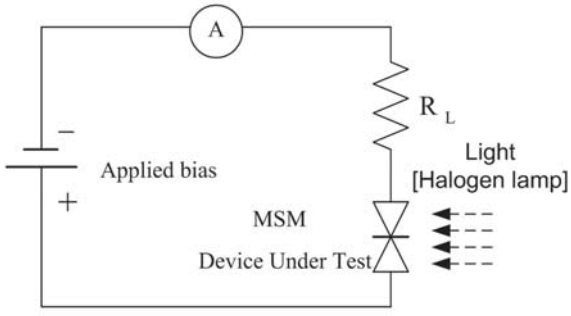

Figure 3 Current-voltage I-V characteristic measurement system.

All measurements were carried out in the temperatures (295-300) °C. The increase in the dark current with applying bias might be attributed to the charge generation in the expanding SCR under reverse bias (Seto, et al., 1997) and/or the incompleteness of fabrication process of the samples.

Results and Discussions

Figure 4 shows the typical photocurrent versus voltage relations at room temperature under different illumination levels from a halogen lamp. Here the photocurrent component was obtained by subtracting the current under dark from the device current at each corresponding bias voltage. Each plot seems to be divided into two regions: the gradually increasing and rapidly increasing regions with bias. Since the present sample has the electrodes widely separated to avoid electronic interference between two junctions, the lateral separated in the depleted region would be more efficient to generate the photocurrent than the residual undepleted neutral region.

This would be the reason why the total photocurrent shows gradual increase with bias. The other region showing rapid increase in the photocurrent above about 12V seems to be under the onset of avalanche breakdown of the Schottky-junction reversed-biased, where the junction on the other side is, of course, forward-biased and it band structure is almost flattened. Under illuminated conditions, however, its saturation character seems to be worse than in the dark.

The reason for this is discussed below in detail. Figure 5 shows the capacitance-voltage (C-V) characteristics of sample as in Fig. 4. Its voltage dependence is rather smaller than the ideal one treated by Sze et al. (Berger, 1996). These results imply that the measured characteristic involves the contribution from the stray capacitance of the measurement unit.

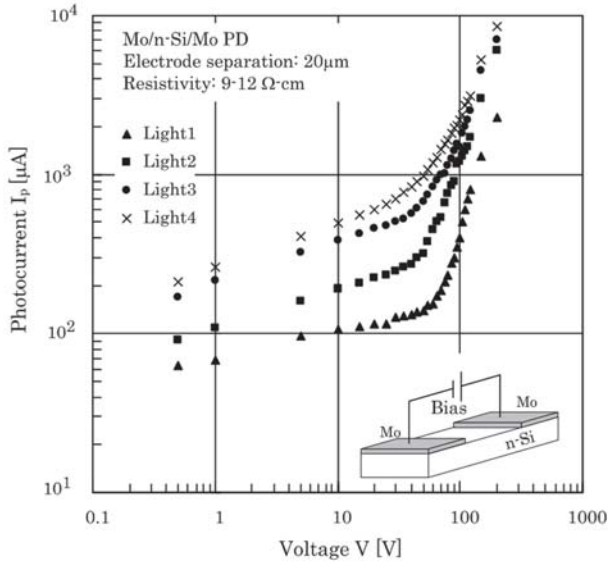

Figure 4 Photocurrent-voltage characteristics of a Mo/n-Si/Mo structure having 20 μm electrode separation.

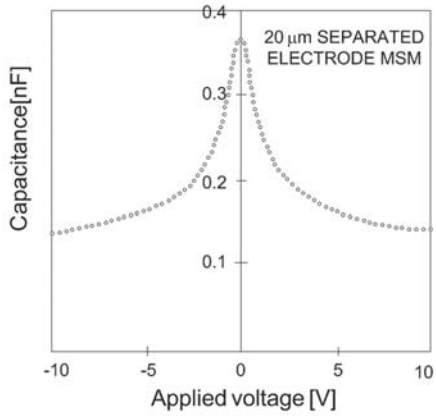

Figure 5 C-V characteristic of the sample appeared in Fig.4.

When a bias voltage is applied between the electrodes, one Schottky-junction is reverse-biased and the other junction is forward-biased. Such a structure is expected to show lateral spreading of its space-charge-region (SCR) at the Schottky-barrier reverse-biased, the spreading of which is possible to be controlled by bias voltage (V). According to the simplified model of such a structure, the width of the lateral spreading *W(V)* of the SCR of the Schottky-junction reverse-biased in the direction of profiling is expressed semi-empirically as (Averine, et al., 2001) and (Masui, et al., 2003).

$$W(V) = \sqrt{\beta(V_{bi} + V)} \qquad (1)$$

with, $\beta = 2\varepsilon_s / qN_D = 16.5\,\mu m^2/V$ and V_{bi} : built-in voltage. A single Schottky-barrier prepared in the same process furnishing a back contact has shown the built-in potential of about 0.23 eV. Therefore, the bias dependence of the SCR width expressed as Eq. (1) is expected to be as shown in Fig. 4 before breakdown bias applied. It is found that, as far as the bias dependence of the plots of the experimental photocurrents concerns, quite similar dependence has been obtained except lower bias regions. In the experimental plots, however, a value bias-independent seems to add to Eq. (1) for each plot. Considering the optical illumination incident onto the whole region between both electrodes, this value is to be the contribution from the diffusion of carriers. Correspondingly, the following experimental (semi-empirical) expression denoting the photocurrent I_P is proposed,

$$I_P = \eta[\alpha W(V) + L] = \eta[\alpha\sqrt{\beta(V + V_{bi})} + L] \qquad (2)$$

Here and are the fitting parameters which can be determined experimentally. The factor η includes the contributions of the size of the active area, the intensity of incident light, and also quantum efficiency. Another parameter α is the effectiveness ratio of the photocurrent generated in the SCR to the current due to the carriers generated in the undepleted region (Takano, et al., 2000) and (Sze, 1981). L is the diffusion length of carriers photoexcited in the undepleted region. As far as Eq.(2) is employed, for a certain sample, the ratio of the value $\alpha\sqrt{\beta}$ to L would be essentially constant.

Another support to the present explanation is the photocurrent behavior observed in the samples made using different resistivity wafers of (9-12) Ω-cm, 23 Ω-cm (40-50) Ω-cm which have 2000 μm electrode separation. Figure 6 shows *Ip-V* characteristics under certain illumination intensity in log-log scale after the contribution of the bias-independent term is excluded.

According to the above consideration, the SCR must be much more efficient in generating photocurrents than the residual undepleted neutral region. To confirm this directly, the photocurrent measurements were performed by moving the irradiating position of the focused beam a He-Ne laser. Figure 7 illustrates the photocurrent distribution profile versus the irradiating position for a 2000 μm electrode separated sample, which was obtained by moving the beam at every

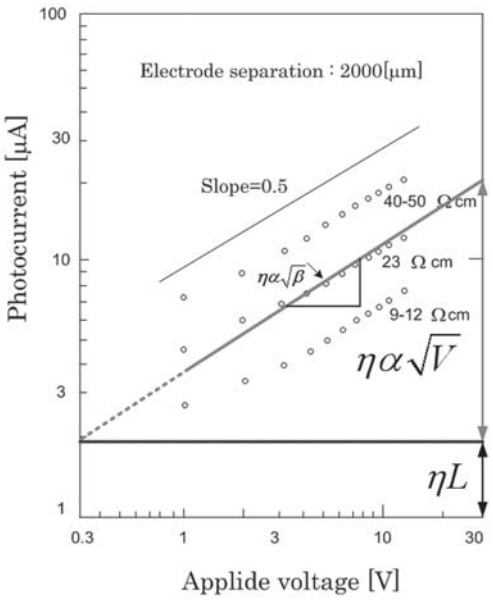

Figure 6 $I_P - V$ characteristics in log-log scale for the samples made on wafers of three different resistivities, (9-12), 23 and (40-50) Ω-cm, which have the same electrode separation of 2000 μm.

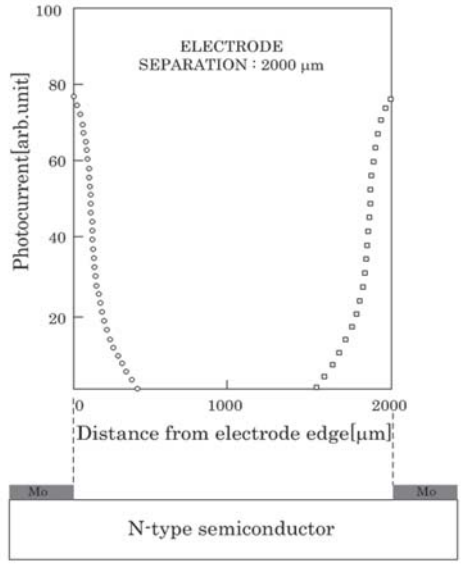

Figure 7 Open circles are for photocurrent profile from the edge of the electrode reverse-biased on the left-hand side. When the sign of bias is reversed, the profile given by open squares is observed. Electrode separation is 2000 μm.

15 μm-step. From this figure, it is apparent that the side of the Schottky barrier reverse-biased can generate appreciable photocurrent. Therefore, it can be mentioned that the SCR is quite efficient in generating photocurrents comparing to the residual undepleted region (Grove, 1967).

To know the potential profile between the electrodes and thus lateral spreading of the SCR, the numerical simulation based on the simplified one-dimensional (1D) model was carried out. As mentioned earlier, the samples having the electrode separation ranging from 20 μm to 2000 μm, where the carrier generation takes place mainly within the absorption depth for 633nm wavelength.

Therefore, quasi-1D model was assumed for the present simulation (Snowden, 1988). Starting from the following two fundamental equations (Selberherr, 1984) the calculations were carried out in the domain size of 1000 μm for computation. The finite difference method followed by the SOR (successive overelaxation)-Newton method was utilized.

One of the two equations is the carrier continuity equation

$$div\left(J_n + J_p\right) + q\frac{d}{dt}\left(p - n\right) = 0\left(t : time\right) \qquad (3)$$

where J_n and J_p are the current densities for electrons and holes, n and p are the electron-and hole-concentrations time-dependent, respectively. The ionized space charge is assumed to be time-independent. Furthermore, by introduction of the source and sink to the electron-current and hole-current, these current components satisfy the following relations,

$$divJ_n - q\frac{dn}{dt} = qR \qquad (4)$$

$$divJ_p - q\frac{dn}{dt} = -qR \qquad (5)$$

where R is the generation and/or recombination rate. Here, since we are treating the process under a steady-state condition, the generation rate and recombination rate were set to be equal. The other equation of the two is the Poisson's equation expressed as,

$$div \cdot grad\,\psi = \frac{q}{\varepsilon_s}\left(n - p - N_D + N_A\right) \qquad (6)$$

where ψ is the potential to be determined across the device, and N_D and N_A are the donor concentration and the acceptor concentration, respectively.

In the numerical calculation, the separation of the electrodes was taken as 1000 μm and carrier generation /recombination rate R under dark was assumed to be $2.9\times10^{17}\ cm^{-3}\ sec^{-1}$. The potential profiles corresponding to several biasing voltages are illustrated in Fig.8. As expected, it is apparent that the width of the SCR along the front surface increases with the bias. Eq.(1) predicts the width of the SCR is about 10 μm at bias of 10V for the present parameters. Although the boundary between the SCR and the undepleted region of the profile in the figure is not clear but the SCR spreading seems to be coincident with the value expected from Eq.(1).

The calculations for larger value of R for illuminated condition were performed, assuming the value of R ten times larger than that of the dark condition. The results revealed that the current level was elevated but the corresponding potential profile itself remained substantially unchanged.

The series resistance of this sample of 1k Ω has been examined from the measurements of the signal response (Takano, et al., 2000). At $I_P = 30\mu A$, for instance, the voltage drop would be 0.038V, which is quite small comparing to the applied biases examined.

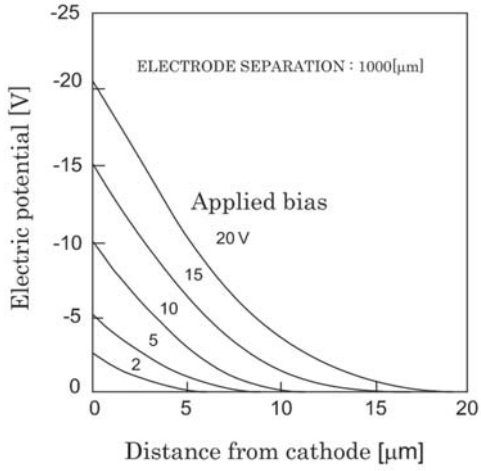

Figure 8 Bias-dependence of potential profiles near the reverse-biased Schottky junction obtained from numerical simulation based on quasi-1D model of 1000 μm -separated electrodes. Generation rate= $2.9\times10^{17}\ cm^{-3}\ sec^{-1}$ was assumed.

The physical parameters used for calculations are given in Table 1.

Conclusion

The laterally spreading of the space-charge-region (SCR) along the surface of planar molybdenum n-type silicon molybdenum structures has been examined experimentally and numerically.

Bias-controllable photocurrent characteristics using planar Mo/n-Si/Mo systems with depleted and undepleted region at the active area were examined and confirmed experimentally. It can be concluded that one can control the photocurrent in a planar MSM structure under dc optical illumination by varying bias. As it were, one can give these structures an electronic iris effect by introducing an undepleted neutral region between electrodes, maintaining the function of changing the optical signal into electronic signal. The neutral region as well as the depleted region plays a key role for this

Table1 : List of symbols and their value used in numerical calculation and in the text

Symbol		Value
V	: applied bias	1-20V
V_{bi}	: built-in voltage of the Mo/n-Si	0.23 eV
$W(V)$	: depletion region width	$\sqrt{[\beta(V_{bi}+V)]}$
$\beta = 2\varepsilon_s / qN_D$		$16.5\mu m^2/V$
ε_s	: permittivity of semiconductor	1.054×10^{-10} F/m
q	: elementary charge	1.60×10^{-19} C
N_D	: donor concentration	$8\times10^{13}\,cm^{-3}$
L	: diffusion length of minorityn carriers	$70\ \mu m$
k	: Effectiveness ratio to undepleted region	2.6

effect. Furthermore, it was revealed that the potential profile and the spreading at the front surface of the SCR of such MSM photodetector structures are approximately but substantially described by the equation semi-empirically proposed based on the simple 1D model.

Acknowledgment

The authors would like to express my deepest gratitude to Prof.Dr. Kazunori Sato and Assoc.ProfDr.Wisut Titiroong- ruang for their valuable comments, advice, and fruitful discussions. Continuous encouragement of Dr.Rutchaneeporn Pookayaporn Phukkamarn of Sripatum University is deeply appreciated. This work was supported in part by The Thailand Research Fund under and Commission Higher Education Grant No. MRG5080004.

References

Averine, S.V.,Chan, Y.C., Lam, Y.L. 2001. "Geometry optimization of interdigitated Schottky-barrier metal-semiconductor-metal photodiode structures." **Solid-State Electron.** 45: 441.

Berger, PR. 1996. "MSM photodiodes." **IEEE Potentials.** Apr/May, Vol. 25.

Grove, As. 1967. **Physics and technology of semiconductor devices.** New York: John Wiley.

Harder, C.S., Van Zeghbroeck, B. J., Kesler, M.P., Meier, H.P., Vettiger, P., Webb, D.J., Wolf P. 1990. "High-speed GaAs/AlGaAs optoelectronic devices for computer applications." **IBM J.Res.Develop, High-speed semiconductor devices.** 34: 568-584.

Masui, T., Khunkhao, S., Kobayashi, K., Niemcharoen, S., Supadech, S., Sato, K.2003. "Photosensing properties of Interdigitated metal semiconductor -metal structures with undepleted region." **Solid-State Electron.** 43: 1811.

Selberherr, S. 1984. **Analysis and simulation of semiconductor devices, Wien Springer-Verlag.** \New York: Wien.

Seto, M., Leduc, J.V., Lammers, MF. 1997. "Al-n-Si Double-Schottky Photodiodes for Optical Storage Systems." 27th ed. European Solid-State Device

Res. Conf. Sept.

Snowden, CM. 1988. **Semiconductor device modeling.** London: Peter Peregrines.

Sze, S.M. 1981. **Physics of semiconductor devices.** New York: John Wiley.

Takano, H., Kimura, H., Ando, T., Niemcharoen, S., Yasumura, Y., Sato K. 2000. "Optical response of planar Mo/n-Si/Mo structures with long neutral region and Schottky barriers at both ends." **Solid-State Electron.** 44: 216.

Wei, C.J., Khul, D., Boettcher, E.H., Bimberg, D., Kuphal, E.1990. "Lateral high-speed metal-semiconductor -metal photodiodes on high-resistivity InGaAs." **IEEE Trans. ED. Lett.** 11: 334.

>> Sanya Khunkhao

Sanya Khunkhao was born in Thailand in 1967. He received the B.S.(Physics) degree from Ramkhamhang University, in 1991, the M.E(Electrical). degree from King Mongkut's Institute of Technology Ladkrabang, Bangkok, Thailand, in 1997, and the D.Eng(Electronics). Degree in electronics engineering from Tokai University, Japan, in April 2005.

He is currently lecturer with Department of Electrical, Faculty of Engineering, Sripatum University and his research interest in Metal-Semiconductor-Metal (MSM) photo detectors base on silicon technology and Electro chromic material.

>> Kazunori Sato

Kazunori Sato received the B.S., M.S. and D.Eng degrees in Electronics engineering from Tokai University, Japan, in 1964, 1966 and 1977, respectively. He is a professor in the Electronics Tokai University. His research interests include Semiconductor Electronics and particularly in semiconductor optical sensors. During 1979-1983, he was with Japanese expert in semiconductor engineering dispatched by Japanese Government to King Mongkut's Institute of Technology Ladkrbang, Bangkok, Thailand, and 2006 to present; he was with Japanese Expert in Electrical and Electronic Engineering dispatched by Japanese Government to Malaysia-Japan University Center, Kuala Lumpur, Malaysia. He was listed in Who's Who in Science and Engineering (2005/2006) (America) and Nominated to Leading Engineers of the World 2006 (England).